THE JOURNAL OF BIOLOGICAL CHEMISTRY VOL. 284, NO. 42, pp. 29218–29229, October 16, 2009

Stomatin-like Protein-1 Interacts with Stomatin and Is Targeted to Late Endosomes*[S]

Received for publication, April 29, 2009, and in revised form, August 19, 2009 Published, JBC Papers in Press, August 20, 2009, DOI 10.1074/jbc.M109.014993

Mario Mairhofer[‡1], **Marianne Steiner**[§], **Ulrich Salzer**[‡], **and Rainer Prohaska**[‡2]

From the [‡]*Max F. Perutz Laboratories, Department of Medical Biochemistry, Medical University of Vienna, Vienna A-1030 and the* [§]*Center for Anatomy and Cell Biology, Department for Nuclear and Developmental Biology and Functional Microscopy, Medical University of Vienna, Vienna A-1090, Austria*

The human stomatin-like protein-1 (SLP-1) is a membrane protein with a characteristic bipartite structure containing a stomatin domain and a sterol carrier protein-2 (SCP-2) domain. This structure suggests a role for SLP-1 in sterol/lipid transfer and transport. Because SLP-1 has not been investigated, we first studied the molecular and cell biological characteristics of the expressed protein. We show here that SLP-1 localizes to the late endosomal compartment, like stomatin. Unlike stomatin, SLP-1 does not localize to the plasma membrane. Overexpression of SLP-1 leads to the redistribution of stomatin from the plasma membrane to late endosomes suggesting a complex formation between these proteins. We found that the targeting of SLP-1 to late endosomes is caused by a G*Y*X*X*Φ (Φ being a bulky, hydrophobic amino acid) sorting signal at the N terminus. Mutation of this signal results in plasma membrane localization. SLP-1 and stomatin co-localize in the late endosomal compartment, they co-immunoprecipitate, thus showing a direct interaction, and they associate with detergent-resistant membranes. In accordance with the proposed lipid transfer function, we show that, under conditions of blocked cholesterol efflux from late endosomes, SLP-1 induces the formation of enlarged, cholesterol-filled, weakly LAMP-2-positive, acidic vesicles in the perinuclear region. This massive cholesterol accumulation clearly depends on the SCP-2 domain of SLP-1, suggesting a role for this domain in cholesterol transfer to late endosomes.

Human stomatin-like protein-1 (SLP-1),[3] also known as STOML-1, STORP (1), slipin-1 (2), or hUNC-24 (3), is the human orthologue of *Caenorhabditis elegans* UNC-24 and a member of the stomatin protein family that comprises 5 human members: stomatin (4–6), SLP-1 (1, 7), SLP-2 (8), SLP-3 (9, 10), and podocin (11). SLP-1 is predominantly expressed in the brain, heart, and skeletal muscle (7, 8) and can be identified in most other tissues (1). Its structure contains a hydrophilic N terminus, a 30-residue hydrophobic domain that is thought to anchor the protein to the cytoplasmic side of the membrane, followed by a stomatin/prohibitin/flotillin/HflK/C (SPFH) domain (12) that is also known as prohibitin (PHB) domain (13), and a C-terminal sterol carrier protein-2 (SCP-2)/nonspecific lipid transfer protein domain (14, 15). This unique structure that was first revealed in *C. elegans* UNC-24 (16) suggests that SLP-1 may be involved in lipid transfer and transport (17).

The founder of the family, stomatin, is a major protein of the red blood cell membrane (band 7.2) and is ubiquitously expressed (18). It is missing in red cells of patients with overhydrated hereditary stomatocytosis, a pathological condition characterized by increased permeability of the red cells for monovalent ions and stomatocytic morphology (19, 20). However, the lack of stomatin is not due to a mutation in its gene but rather to a transport defect (21, 22). Stomatin is a monotopic, oligomeric, palmitoylated, cholesterol-binding membrane protein (18) that is associated with lipid rafts (23, 24) or raft-like detergent-resistant membranes (DRMs) (25), serving as a respective marker (26–28). Other stomatin family members like podocin (29, 30) and SLP-3 (9) are also enriched in DRMs. Many SPFH/PHB proteins share this property suggesting that the SPFH/PHB domain plays an important role in lipid raft/DRM targeting (13, 31). Several interactions of stomatin with membrane proteins have been revealed, notably with the acid sensing ion channels (32) and the glucose transporter GLUT1 (33, 34). Interestingly, stomatin functions as a switch of GLUT1 specificity from glucose to dehydroascorbate in the human red blood cell thus increasing vitamin C recycling and compensating the human inability to synthesize vitamin C (35).

The *C. elegans* genome contains 10 members of the stomatin family. Defects in three of these genes (*mec-2, unc-1*, and *unc-24*) cause distinct neuropathologic phenotypes, namely uncoordinated movement and defect in mechanosensation, respectively (36, 37). These are explained by dysfunction of the respective stomatin-like proteins in complex with degenerin/epithelial sodium channels that also affects the sensitivity to volatile anesthetics (38, 39). Importantly, MEC-2 and human podocin bind cholesterol and form large supercomplexes with various ion channels thus modulating channel activity (40). The biological functions of the SLP-1 orthologue UNC-24 and stomatin orthologue UNC-1 are associated, because the *unc-24* gene controls the distribution or stability of the UNC-1 protein (41). In addition, UNC-24 co-localizes and interacts with

* This work was supported by grants from the Austrian Science Fund/Fonds zur Foerderung der wissenschaftlichen Forschung (FWF).

[S] The on-line version of this article (available at http://www.jbc.org) contains supplemental Figs. S1–S6.

[1] Present address: Dept. of Obstetrics and Gynecology, Medical University of Vienna, Vienna A-1090, Austria.

[2] To whom correspondence should be addressed: Dr. Bohr-Gasse 9/3, Vienna A-1030, Austria. Tel.: 43-1-4277-61660; Fax: 43-1-4277-9616; E-mail: rainer.prohaska@meduniwien.ac.at.

[3] The abbreviations used are: SLP-1, stomatin-like protein 1; DRM, detergent-resistant membrane; LAMP, lysosomal-associated membrane protein; PHB, prohibitin; SCP-2, sterol carrier protein 2; SPFH, stomatin/prohibitin/flotillin/HflC/K; TfR, transferrin receptor; TRITC, tetramethylrhodamine isothiocyanate; WT, wild type; GFP, green fluorescent protein; HA, hemagglutinin; PBS, phosphate-buffered saline.

MEC-2 and is essential for touch sensitivity (36). Based on these observations, we hypothesize that human stomatin and SLP-1 similarly interact and modify the distribution of each other. These proteins may have important functions in regulating the activity of ion channels in the human brain and muscle tissues. Despite its putative role in cellular lipid distribution, SLP-1 has not been studied to date.

In this work, we characterized human SLP-1 as a late endosomal protein and identified an N-terminal GY*XX*Φ motif as the targeting signal. We found that SLP-1 interacts with stomatin *in vitro* and *in vivo* and associates with DRMs. Regarding the proposed lipid transfer function, we showed that SLP-1 induces the formation of large, cholesterol-rich vesicles or vacuoles when cholesterol trafficking from the late endosomes is blocked suggesting a net cholesterol transfer to the late endosomes and/or lysosomes. This effect was clearly attributed to the SCP-2/nonspecific lipid transfer protein domain of SLP-1, in line with the original hypothesis.

EXPERIMENTAL PROCEDURES

Antibodies and Reagents—The monoclonal antibody against human stomatin (GARP-50) was described previously (5). Monoclonal antibodies against LAMP-1 (clone H4A3) and LAMP-2 (clone H4B4) were from the Developmental Studies Hybridoma Bank (University of Iowa), the rabbit polyclonal and mouse monoclonal (clone 4A6) antibodies against the myc tag were from Upstate. Monoclonal antibody against flotillin-2 was from BD Transduction Laboratories; monoclonal antibody against cation-independent mannose 6-phosphate receptor (clone 2G11), and rabbit antibody against GFP were from Abcam. Monoclonal antibody against GFP (clone B2) and rabbit antibody against the transferrin receptor (TfR) were obtained from Santa Cruz. Fluorescent secondary antibodies (anti-mouse Alexa 488, anti-rabbit Alexa 488, anti-mouse Alexa 596, and anti-rabbit Alexa 596) and LysoTracker Red were from Molecular Probes/Invitrogen. Purified recombinant GFP protein was from Upstate; Dulbecco's modified Eagle's medium, fetal bovine serum, antibiotics, and glutamate stocks were purchased from PAA Laboratories, Inc. (Pasching, Austria). Filipin and TRITC-dextran were from Sigma; U18666A was from Calbiochem.

Preparation of Tagged SLP-1 and Rab Constructs—IMAGE-clone number 5185908 carrying the complete coding region for the SLP-1 protein was obtained from the German Resource Center for Genome Research (RZPD). The coding region was amplified by PCR from the vector with the following primers: SLP-1-GFP-NT, CGGAATTCGCCATGCTCGGCAGGTCT and SLP-1-GFP-CT, TCCCCGCGGCTGCGCCCTTCAAGGCCCTGAGGAC. PCR products were digested with restriction enzymes EcoRI and SacII and ligated into the corresponding sites of the pEGFP-N3 vector (BD Biosciences Clontech). To yield myc-tagged SLP-1, a double-stranded oligonucleotide coding for sequence EQKLISEEDL and followed by a stop codon was ligated into the SpeI and EcoRV restriction sites of the pEFBOS-puro vector. The coding region of SLP-1 was amplified by PCR with primers SLP-1-myc-NT, GGACTAGTGCCATGCTCGGCAGGTCT and SLP-1-myc-CT, GGACTAGTCTTCAAGGCCCTGAGGAC, the PCR product was digested with SpeI and ligated into the SpeI restriction site preceding the myc tag. C-terminal deletions SLP-1-(1–288)-GFP and SLP-1-(1–224)-GFP were constructed using SLP-1-GFP-NT as forward primer and the respective reverse primers for PCR: SLP1-T288-GFP, TCCCCGCGGCTGCGCCAGGCTGCTTCGGACTGG and SLP1-T224-GFP, TCCCCGCGGCTGCGCCCGGCTGGAGCACGGCCTC. N-terminal deletions were constructed by PCR amplification with the SLP-1-myc-CT reverse primer and the following forward primers: SLP-1-(43–397)-myc, GGACTAGTCCACCATGGCCGATGTACCCCAGAGC and SLP-1-(11–397)-myc, GGACTAGTCCACCATGCTGGGTGATTTTGACCGC. An overview of the SLP-1 deletion mutants and tagged constructs used in this work are given in Fig. 1. The point mutation Y6A in the GY*XX*Φ motif was introduced by PCR with the mutagenic forward primer: GGACTAGTCCACCATGCTCGGCAGGCTTGGGGCCCGGGCGCTGCC and the SLP-1-myc-CT primer. The PCR product was digested with SpeI and ligated into the XbaI site of vector pC3HA (based on pcDNA3.1hygro) upstream of a triple HA tag. The point mutation L9S was introduced by amplifying the region between the KpnI and BamHI restriction sites in the SLP-1 coding sequence with the mutagenic 5′ primer, GGTCTGGGTACCGGGCGTCCCCCCTGGGTGATTTTGACC and the non-mutagenic 3′ primer, GCGGATCCGGCCCAGG. This mutagenized fragment was then inserted into the SLP-1-myc construct via these restriction sites, giving rise to SLP-1(L9S)-myc. The chimeric SLP-1-stomatin fusions

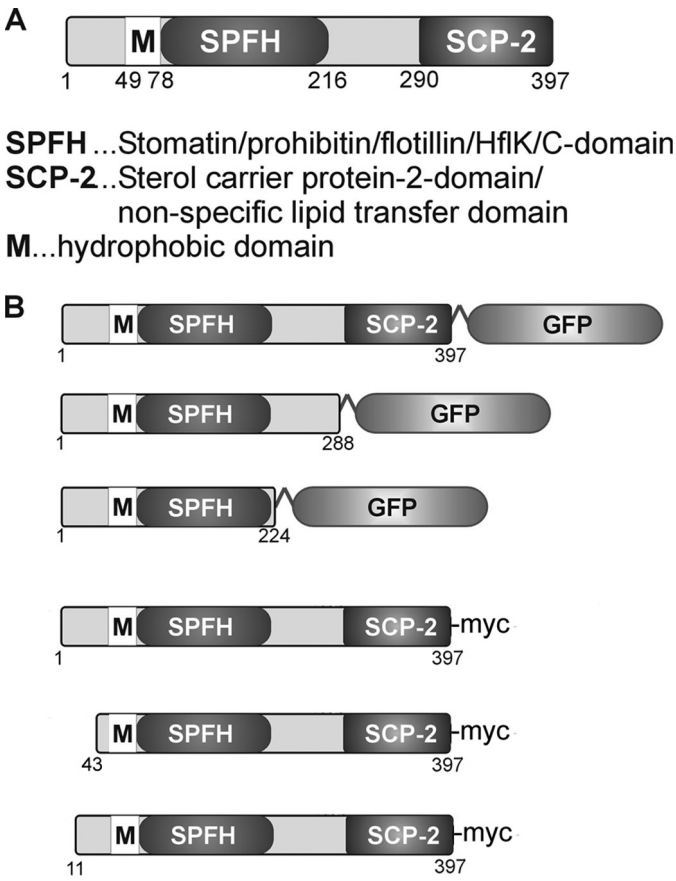

FIGURE 1. *A*, schematic representation of the domain structure of SLP-1. *B*, SLP-1 constructs used in this study.

were prepared as follows. The coding region for amino acids 1–49 was amplified either from WT or Y6A or L9S mutated SLP-1 with the following primers: SLP-1-GFP-NT forward and the SLP-1-(1–49)-CT reverse primer with a SacII restriction site, TCCCCGCGGCTGCGCCGCTCTGGGGTACATCGG, and were inserted into the pEGFP-N3 vector. Then, the STOM-(21–287)-GFP construct (42) was digested with EcoRI, blunted with Klenow polymerase, and digested with BglII. The inserts with the coding region for amino acids 1–49 of SLP-1 (or point mutants Y6A or L9S) were prepared by digestion with SacII, followed by Klenow incubation, heat inactivation of Klenow enzyme, and subsequent digestion with BglII. The ligation of this insert into the STOM-(21–287)-GFP vector yields an in-frame fusion of the WT or point-mutated N terminus of SLP-1 to the N-terminal-truncated stomatin construct, with an 8-amino acid linker (GAANSATM) between the two sequences. Clones carrying the coding sequences for the different Rab proteins in a pcDNA3.1+ vector were purchased from the Missouri S&T cDNA Resource Center. The coding regions were amplified with primers: GFP-Rab5Aforw, GCCGCTCGAGGCGCTAGTCGAGGCGCA; GFP-Rab5Arev, CGGGGTACCTTAGTTACTACAACACTGA; GFP-Rab7Forw, GCCGCTCGAGGCACCTCTAGGAAGAAAG, GFP-Rab7Rev, CGGGGTACCTCAGCAACTGCAGCTTTCT; GFP-Rab9Forw, GCCGCTCGAGGCGCAGGAAAATCTTCAC; and GFP-Rab9Rev, CGGGGTACCTCAACAGCAAGATGAGCTA. PCR products were digested with XhoI and KpnI and ligated into the pEGFP-C1 vector (BD Biosciences Clontech).

Cell Culture and Transfections—HeLa cells, HepG2 cells, and Madin-Darby canine kidney cells were routinely maintained in Dulbecco's modified Eagle's medium, 10% fetal bovine serum supplemented with 100 units/ml penicillin and streptomycin under standard conditions. About 5×10^5 cells per well were seeded on 6-well plates, cultivated overnight, and transient transfections were performed with Lipofectamine 2000 (Invitrogen) according to the manufacturer's instructions. To obtain cell lines stably expressing tagged fusion proteins, transiently transfected cells were trypsinized and transferred to 100-mm culture dishes. The next day, either puromycin (2 μg/ml) or G418 (700 μg/ml) were added and the cells were cultured for 2–3 weeks until large single clones were visible. Multiple clones were picked with cloning rings (Sigma), expanded, and analyzed for expression of tagged fusion proteins by Western blotting and immunofluorescence microscopy. Cells with high and low expression levels were maintained.

Immunoelectron Microscopy—HeLa cells stably expressing SLP-1-GFP were grown on gridded Cellocate coverslips (Eppendorf). Cells strongly expressing SLP-1-GFP were selected and phase-contrast and fluorescence images were recorded. Subsequently, the cells were fixed for 1 h in 0.1 M sodium phosphate buffer, pH 7.4, containing 4% paraformaldehyde and 0.2% glutaraldehyde, washed for 30 min with 0.1 M phosphate buffer, and then incubated for 2 h in 0.1 M phosphate buffer containing 50 mM glycine. Embedding in LR White, trimming, and thin sectioning was essentially performed as described (43). Thin sections were blocked for 1 h in phosphate-buffered saline (PBS), pH 7.4, containing 0.05% Tween 20, 5% bovine serum albumin, and 1% goat serum. Rabbit anti-GFP (Abcam) was diluted 1/500 in blocking buffer and thin sections were incubated for 2–3 h at room temperature. After washing 3 times with PBS, pH 7.4, 0.05% Tween 20, the thin sections were incubated with a 10-nm gold-conjugated goat anti-rabbit antibody (Biocell; diluted 1/40 in PBS, pH 8.0, 0.05% Tween 20) for 2 h. Finally, the thin sections were washed 3 times with PBS, pH 8.0, 0.05% Tween 20, stained with 2% uranyl acetate for 1 h and then analyzed with a Jeol 1200 EXII microscope. Staining of thin sections with blocked anti-GFP (incubated with a 10-fold excess of recombinant GFP for 2 h, 37 °C) showed only minimal background.

Fluorescence Microscopy—Immunofluorescence microscopy was performed as described (42) except that the paraformaldehyde concentration in the fixing solution was 4%. In some experiments, lysosomes/late endosomes were stained with LysoTracker Red (Invitrogen) according to the manufacturer's instructions. For internalization of TRITC-dextran, cells were serum-starved overnight and then incubated at 37 °C in phenol red-free Dulbecco's modified Eagle's medium, 10% fetal calf serum, 5 mg/ml TRITC-dextran for 10 min. After labeling, cells were washed twice with PBS and fixed for fluorescence microscopy or incubated for 30 min in the same medium without TRITC-dextran prior to fixation.

Isolation of DRMs—HeLa cells stably expressing SLP-1-GFP or GFP-tagged C-terminal truncation mutants of SLP-1 were grown in 150-mm culture dishes. Two dishes were used for each flotation experiment. Isolation of cellular membranes and subsequent density gradient centrifugation was performed as described (28) with some modifications. In brief, the resulting postnuclear supernatant was transferred to a SW55 polyallomer centrifuge tube (Beckman), diluted with 2 volumes of homogenization buffer (250 mM sucrose, 3 mM imidazole, pH 7.4, with added protease inhibitors aprotinin, leupeptin, pepstatin A, and 4-(2-aminoethyl)benzenesulfonyl fluoride), and centrifuged at 100,000 $\times$ *g* for 30 min to pellet cellular membranes. The membrane pellet was resuspended in 500 μl of ice-cold lysis buffer (1% Triton X-100, 150 mM NaCl, 10 mM Tris-Cl, pH 7.4, 5 mM EGTA, and protease inhibitors), lysed for 15–20 min on ice, and then mixed with 800 μl of 80% sucrose in Tris-buffered saline, pH 7.4. After complete mixing, 1.2 ml of the lysate, now containing 50% sucrose, were transferred to the bottom of a SW55 centrifuge tube, overlaid with 0.8 ml of 40% sucrose in Tris-buffered saline, 2 ml of 35% sucrose in Tris-buffered saline, and 0.5 ml of 5% sucrose in Tris-buffered saline. The gradient was centrifuged for 16–18 h at 230,000 $\times$ *g* in a Beckman ultracentrifuge with a SW55 rotor. Nine fractions of 0.5 ml were collected from the top and analyzed by SDS-PAGE and Western blotting. Aliquots of the gradient fractions were analyzed for protein (B_D protein determination kit, Bio-Rad) and cholesterol (Infinity cholesterol determination kit, Thermo Electron).

Subcellular Fractionation on Opti-Prep Gradients—Fractionation of HeLa cell lysates on Opti-Prep gradients was performed as described (44), with some modifications. In brief, one 150-mm dish with confluent cells was used for preparing lysates. A post-nuclear supernatant was prepared as described above. One ml of this supernatant was loaded on top of an

11-ml linear density gradient from 5 to 20% Opti-Prep (containing 250 mM sucrose, 3 mM imidazole, pH 7.4, and 1 mM EDTA) prepared in a SW40 centrifuge tube and centrifuged at 100,000 × *g* for 14–16 h. Nineteen fractions of 580 μl were taken from the top and analyzed by SDS-PAGE and Western blotting. Aliquots were assayed for alkaline phosphatase activity as described (45).

Immunoprecipitation—HeLa cells stably expressing GFP fusion proteins were lysed in RIPA buffer and immunoprecipitation was performed by a standard protocol (46). Rabbit anti-GFP antibody was used for specific reactions; rabbit preimmune serum was used for the control. The immunoprecipitates were analyzed by SDS-PAGE and Western blotting using the respective mouse monoclonal antibodies. Control HeLa cells and HeLa cells stably expressing GFP alone were used as further controls to make sure that co-immunoprecipitation of endogenous stomatin is not due to unspecific binding to the polyclonal antibody. In both controls, no stomatin was precipitated with the anti-GFP antibody (data not shown).

Blocking Intracellular Cholesterol Transport with the Amino Steroid U18666A—A mixture of control HeLa cells and HeLa cells stably expressing the respective fusion protein was seeded onto glass coverslips at about 50% density. Cells were left to adhere overnight and the indicated concentrations of U18666A were added from a 2 mg/ml stock solution in water. Accumulation of cholesterol in perinuclear vesicles was assessed by filipin staining as described (47).

RESULTS

SLP-1 Is Targeted to Perinuclear Multivesicular Bodies in Different Cell Types—Due to the lack of antibodies against native SLP-1, we prepared myc-, HA-, and GFP-tagged SLP-1 constructs, expressed them transiently and stably in several cell lines, and analyzed the cells by confocal microscopy. Fig. 2*A* depicts a HeLa cell stably expressing SLP-1-myc, a HepG2 cell transiently expressing SLP-1-GFP, and a Madin-Darby canine kidney cell transiently expressing SLP-1-GFP. In all 3 cell types, we observed perinuclear vesicle staining as for stomatin (48). The same pattern was observed with HA-tagged SLP-1 (data not shown). In contrast to stomatin, we did not see any plasma membrane staining, neither in low expressing nor highly overexpressing cells. Immunoelectron microscopy of HeLa cells stably expressing SLP-1-GFP showed mainly staining of the limiting membrane of multivesicular bodies (Fig. 2*B*). These data suggest that SLP-1 is targeted to the late endosomal compartment.

SLP-1 Co-localizes with Markers of the Late Endosomal Compartment—We performed immunofluorescence and confocal microscopy of HeLa cells stably expressing either SLP-1-GFP or SLP-1-myc and co-stained them with antibodies against early and late endosomal markers. SLP-1 co-localized with the late endosomal marker LAMP-2 and partially with cation-independent mannose 6-phosphate receptor, a marker for a late endosomal subset (Fig. 3*A*). In contrast, no co-localization was observed with TfR, a marker for early/recycling endosomes. Moreover, we transiently transfected SLP-1-myc expressing HeLa cells with GFP-tagged Rab5A, Rab7, and Rab9 to visualize early (Rab5) and late (Rab7, Rab9) endosomes. SLP-1 clearly co-localized with Rab7 and Rab9 but not with Rab5 (Fig. 3*B* and supplemental Fig. S1*A*). Neither markers for the Golgi apparatus (GM130) nor peroxisomes (PMP70) co-localized with SLP-1 (supplemental Fig. S1*B*). To functionally confirm the late endosomal localization of SLP-1, we performed internalization studies with TRITC-dextran. After a 10-min incubation with TRITC-dextran, no co-localization with SLP-1-GFP was observed but after a chase time of 30 min, some SLP-1-GFP-positive vesicles were clearly labeled with endo-

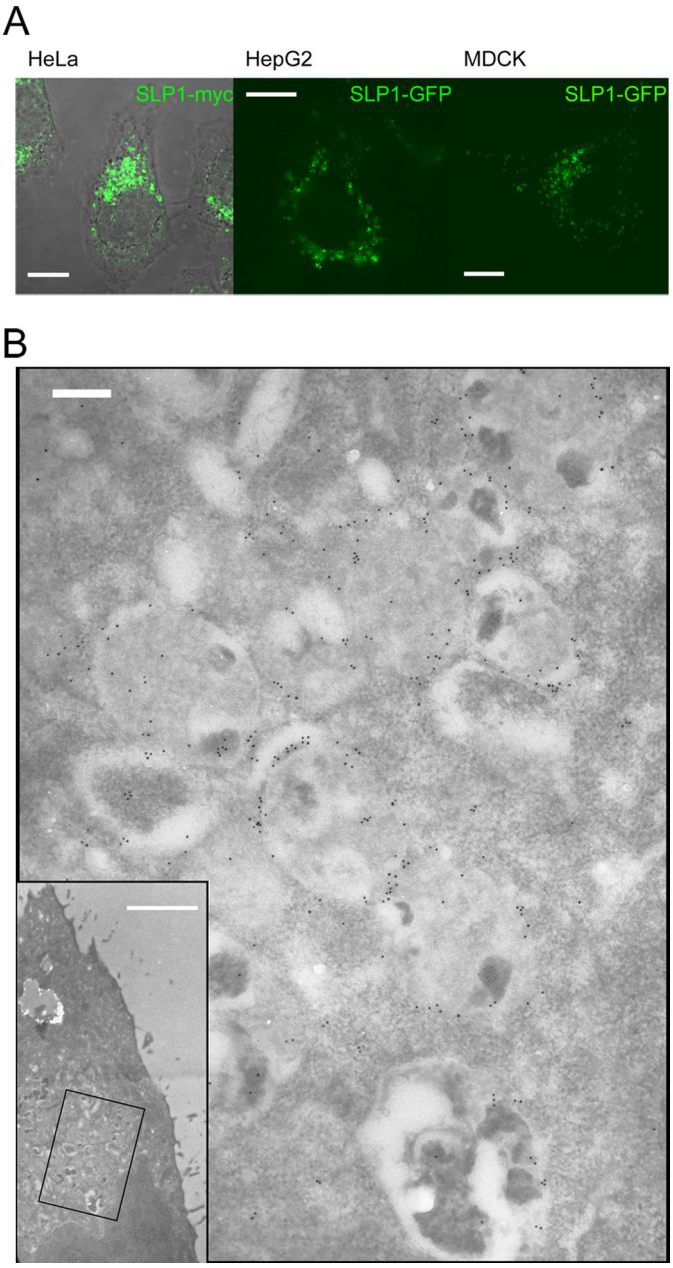

FIGURE 2. **SLP-1 is localized to perinuclear, multivesicular bodies.** *A*, HeLa, HepG2, and Madin-Darby canine kidney (*MDCK*) cells were transiently transfected with SLP-1-myc or SLP-1-GFP constructs, as indicated. Cells were fixed and processed for confocal microscopy. Perinuclear staining was observed in all 3 cell types. *Scale bars*, 10 μm. *B*, immunoelectron micrographs of a HeLa cell stably expressing SLP-1-GFP. Thin sections were incubated with anti-GFP and 10-nm immunogold conjugates and counterstained with uranyl acetate. The *inset* shows a low magnification picture of the cell (*scale bar*, 2 μm), the *boxed region* is shown at high magnification. SLP-1-GFP is detected on the limiting membrane of multivesicular bodies. *Scale bar*, 200 nm.

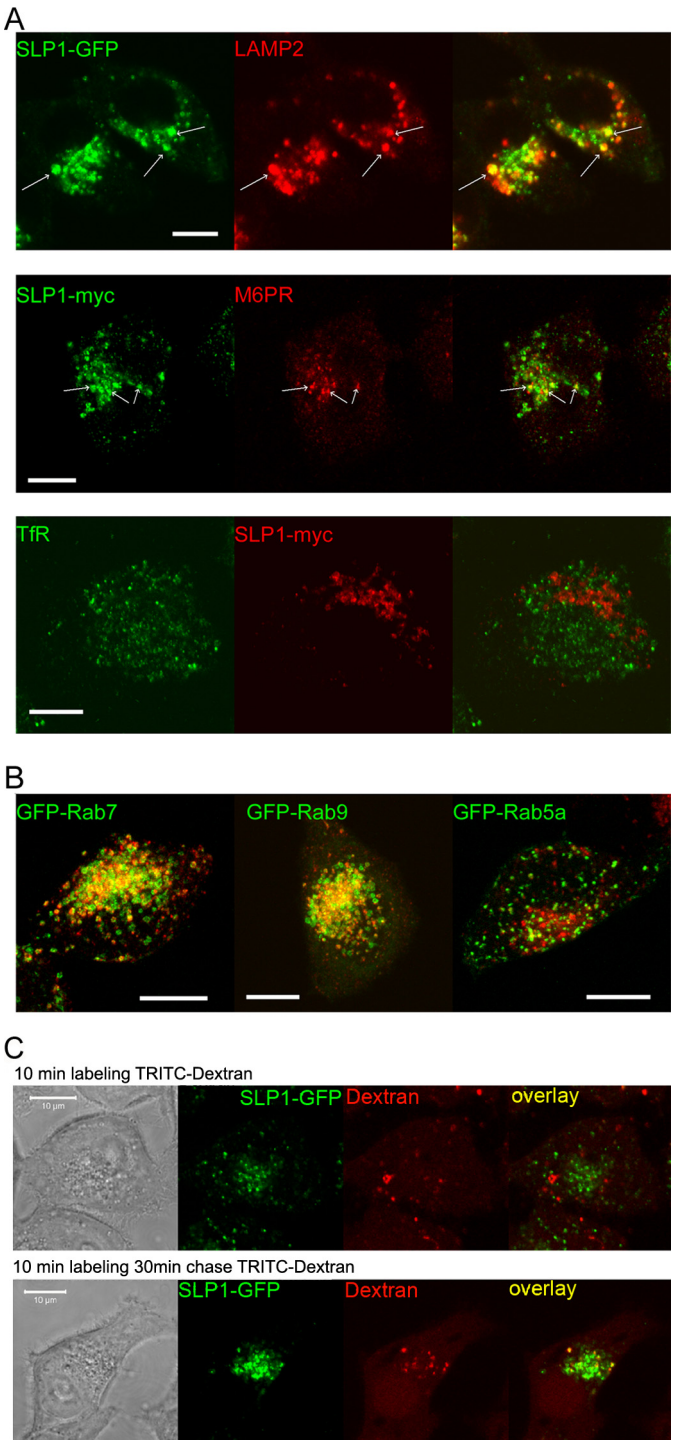

FIGURE 3. **SLP-1 co-localizes with late endosomal markers.** *A*, HeLa cells stably expressing SLP-1-GFP or SLP-1-myc were co-stained with the indicated marker antibodies and analyzed by confocal microscopy. Partial co-localization with LAMP-2 and cation-independent mannose 6-phosphate receptor (*M6PR*) was detected. Some clearly double-stained vesicles are marked by *arrows*. No co-localization was observed with the early/recycling endosomal marker TfR. *B*, HeLa cells stably expressing SLP-1-myc were transiently transfected with the indicated GFP-Rab fusion constructs. Cells were seeded onto glass coverslips, fixed about 48 h after transfection, and stained with anti-myc antibody. *Z*-stacks of cells expressing the GFP-Rab fusion proteins and SLP-1-myc were recorded with the Zeiss LSM 510 Meta confocal microscope. Projections of the *Z*-stacks onto the XY-plane are shown. An overlay of the *green* and *red channels* of this projection is shown for GFP-Rab7, GFP-Rab9, and GFP-Rab5, respectively. Single channel images can be viewed in supplemental Fig. S1*A*. The *yellow* color in the overlays reveals co-localization of SLP-1 with GFP-Rab7 and GFP-Rab9, respectively. Only very little co-localization is observed for GFP-Rab5. *C*, HeLa cells stably expressing SLP-1-GFP were incubated with TRITC-dextran for 10 min, washed, and fixed immediately (*upper panel*) or chased for 30 min before fixation (*lower panel*). No co-localization of SLP-1-GFP and TRITC-dextran was observed after 10 min of endocytosis, although clearly double-labeled structures were observed after a 30-min chase thus indicating that SLP-1 resides in late endosomes accessible to endocytosed material. *Scale bars*, 10 μm.

cytosed, fluorescent dextran (Fig. 3*C*) verifying the late endosomal localization.

Overexpression of SLP-1 Causes Redistribution of Stomatin from the Plasma Membrane to the Late Endosomal Compartment—Because of the late endosomal localization of both stomatin and SLP-1, we transiently transfected HeLa cells with myc- or GFP-tagged SLP-1 and analyzed their co-distribution with endogenous stomatin. In untransfected cells, stomatin showed plasma membrane and perinuclear staining as reported previously (28). In cells expressing SLP-1, stomatin and SLP-1 co-localized in perinuclear vesicles (Fig. 4*A*, *upper panel*). A shift of stomatin distribution from the plasma membrane to perinuclear vesicles was observed suggesting an interaction of these proteins. This effect was quantified by fluorescence intensity scanning through normal and SLP-1-myc-expressing HeLa cells (Fig. 4*A*, *lower panels*). To confirm this finding biochemically, we performed subcellular fractionation of these cells and compared the distribution of stomatin. Concomitantly, the distribution of alkaline phosphatase, a plasma membrane marker, and LAMP-1, a late endosomal/lysosomal marker, was determined. The alkaline phosphatase plasma membrane pool was assigned to gradient fractions 2–6 (Fig. 4*B*), whereas LAMP-1 positive endosomes were broadly distributed in dense fractions 7–13 (Fig. 4*C*, *upper panel*). SLP-1-myc and the C-terminal truncation mutant SLP-1-(1–288)-GFP were only found in dense fractions co-distributing with LAMP-1, whereas the N-terminal truncation SLP-1-(43–397)-myc was also found in plasma membrane fractions (Fig. 4*C*, *middle panel*). Stomatin was distributed in plasma membrane and endosomal fractions of control HeLa cells, however, in SLP-1-myc expressing cells, a shift of stomatin from the plasma membrane to endosomal fractions was observed (Fig. 4*C*, *lower panel*) in accordance with the microscopic data. A similar result was obtained for SLP-1-(1–288)-GFP expressing cells, whereas SLP-1-(43–397)-myc expression had little effect on stomatin distribution (Fig. 4*C*, *lower panel*). A quantitative representation of these results is shown in Fig. 4*D*. Together, these data indicate that overexpression of SLP-1 induces redistribution of stomatin from the plasma membrane to the late endosomal compartment.

Endogenous Stomatin Is Co-immunoprecipitated with SLP-1 and C-terminal Truncation Mutants of SLP-1—To identify the interaction between SLP-1 and stomatin and to estimate the binding region of SLP-1, we co-immunoprecipitated endogenous stomatin with SLP-1-GFP, SLP-1-(1–288)-GFP, and SLP-1-(1–224)-GFP, respectively (Fig. 5). Stomatin co-precipitated with both SLP-1-GFP and SLP-1-(1–288)-GFP (Fig. 5*A*), thus showing that the SCP-2-domain or C-terminal end is not involved in this interaction. There was less stomatin precipitating with SLP-1-(1–224)-GFP, however, in contrast to the other proteins, this mutant shows different subcellular targeting (supplemental Fig. S2). The input and supernatants of the pre-

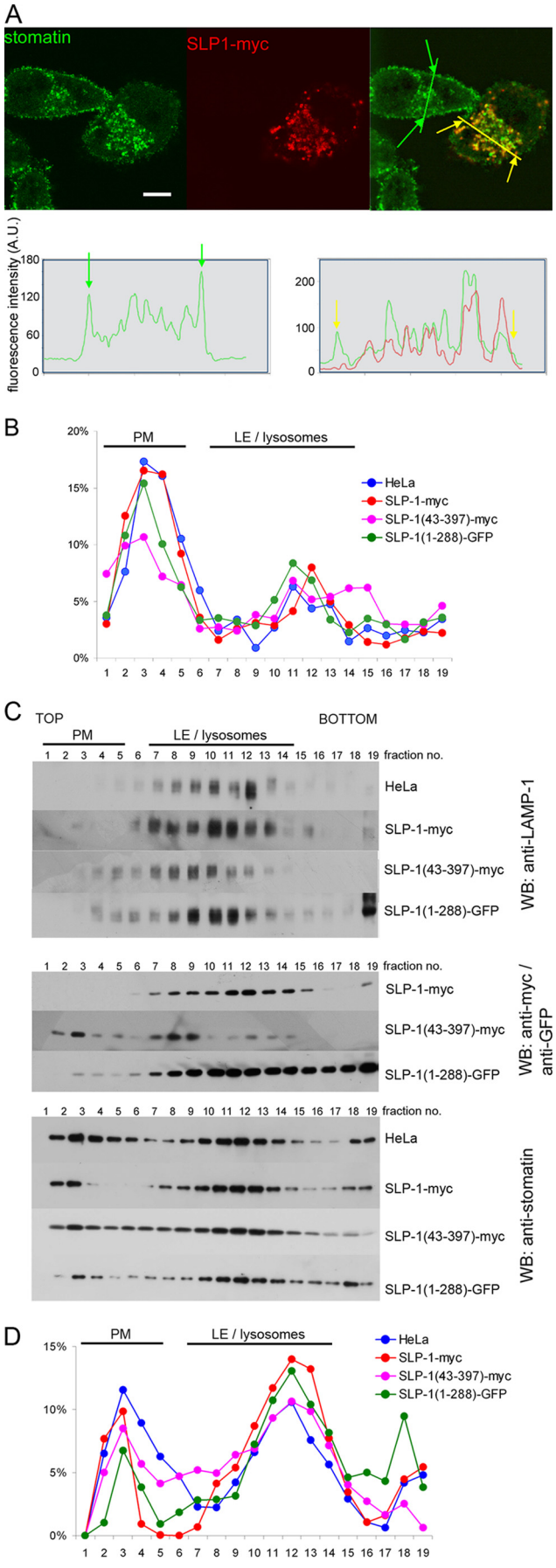

cipitations are shown in Fig. 5*B*. An estimated 30% of stomatin were co-precipitated with SLP-1-GFP. These results show that SLP-1 forms a complex with stomatin and that, in contrast to stomatin, the distal C-terminal region of SLP-1 was not involved in this complex formation.

SLP-1 and the C-terminal Deletion Mutants SLP-1-(1–288) and SLP-1-(1–224) Are Enriched in DRMs—Based on the biochemical similarities of SLP-1 and stomatin, we expected their co-localization in DRMs. Therefore we analyzed the flotation behavior of SLP-1-GFP and stomatin (Fig. 6, *upper panel*). SLP-1-GFP was detected in DRM fractions 1–2 but also in high-density fractions representing solubilized protein. The distribution of stomatin was almost identical. The DRM marker flotillin-2 was present in DRM fractions, whereas the non-raft marker TfR was found in high-density fractions. DRM fractions were enriched in cholesterol but contained only 5–6% of total protein (Fig. 6, *lower panel*). In relation to the total protein content, SLP-1-GFP was strongly enriched in the DRMs. The C-terminal deletion mutants SLP-1-(1–288)-GFP and SLP-1-(1–224)-GFP were also enriched in DRM fractions and co-distributed with stomatin (supplemental Fig. S3). This result is in marked contrast to stomatin deletions or point mutations near the C-terminal end that abolish DRM association (49).

A GYXXΦ Motif in the N-terminal Domain of SLP-1 Functions as a Late Endosomal Targeting Signal—Sequence analysis of the SLP-1 N terminus revealed a potential Y-based targeting motif, GYRAL (residues 5–9), which meets the GY*XX*Φ consensus sequence (Φ being a bulky, hydrophobic amino acid) that is essential for sorting lysosomal proteins (50). Accordingly, deletion of residues 1–10 or 1–42, containing the GY*XX*Φ motif, abolished late endosomal targeting and caused strong plasma membrane staining (Fig. 7). Point mutations of Tyr-6 (Y6A) and Leu-9 (L9S) also caused plasma membrane accumulation of these mutants (Fig. 7, *lower panels*) confirming that GY*XX*Φ is essential for the late endosomal targeting.

FIGURE 4. **Overexpressed SLP-1 co-localizes with endogenous stomatin and modifies its subcellular distribution.** *A*, HeLa cells were transiently transfected with SLP-1-myc (*upper panel*). In cells strongly expressing SLP-1-myc, endogenous stomatin immunofluorescence on the plasma membrane is markedly reduced when compared with non-expressing HeLa cells. Co-localization of SLP-1-myc and stomatin on perinuclear vesicles is clearly observed. The intracellular distribution of stomatin in a non-expressing cell was compared with a strongly SLP-1-myc expressing cell (*lower panel*). Intensity profiles for the *green* and *yellow lines* in the overlay image were obtained with ImageJ. *Green* and *yellow arrows* mark the position of the plasma membrane on the overlay image and on the intensity profiles. Please note the relative reduction of the stomatin signal on the plasma membrane in the SLP-1-myc expressing cell compared with the non-expressing cell. *Scale bars*, 10 μm. *B*, control HeLa cells and HeLa cells stably expressing the indicated SLP-1 constructs were analyzed by subcellular fractionation on 5–20% OptiPrep density gradients. The diagram shows the relative distribution of the plasma membrane (*PM*) marker alkaline phosphatase along the 19 gradient fractions. The major alkaline phosphatase activity was detected in fractions 2–5. *C*, the distribution of LAMP-1 (*upper panel*), the different SLP-1 constructs (*middle panel*), and stomatin (*lower panel*) in control HeLa cells and cells stably expressing the indicated constructs was analyzed by Western blotting. Fractions containing markers for plasma membrane or late endosomes (*LE*)/lysosomes are indicated. *D*, quantitative analysis of the stomatin Western blots was performed with ImageJ. The relative distribution of stomatin along the gradient fractions is compared for normal HeLa cells and stable clones expressing the indicated constructs.

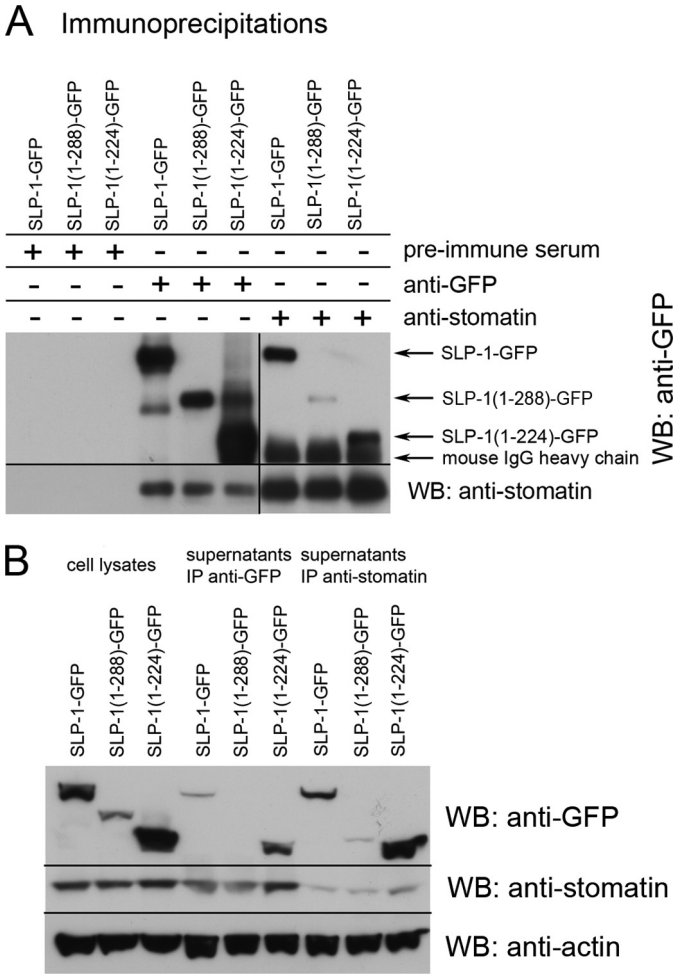

FIGURE 5. **Stomatin forms a complex with SLP-1 and C-terminal-truncated SLP-1.** *A*, HeLa cells stably expressing the indicated constructs were lysed with RIPA buffer. Rabbit anti-GFP serum was used to precipitate the SLP-1-GFP constructs; preimmune rabbit serum was used as nonspecific control. Endogenous stomatin was precipitated with the mouse monoclonal antibody GARP50. For Western blotting (*WB*), the indicated monoclonal antibodies were used. *B*, comparison of the cell lysates and the immunoprecipitated supernatants. Equal amounts of the RIPA cell lysates and immunoprecipitated supernatants were analyzed by SDS-PAGE and Western blotting with the indicated antibodies. Actin was used as loading control. *IP*, immunoprecipitation.

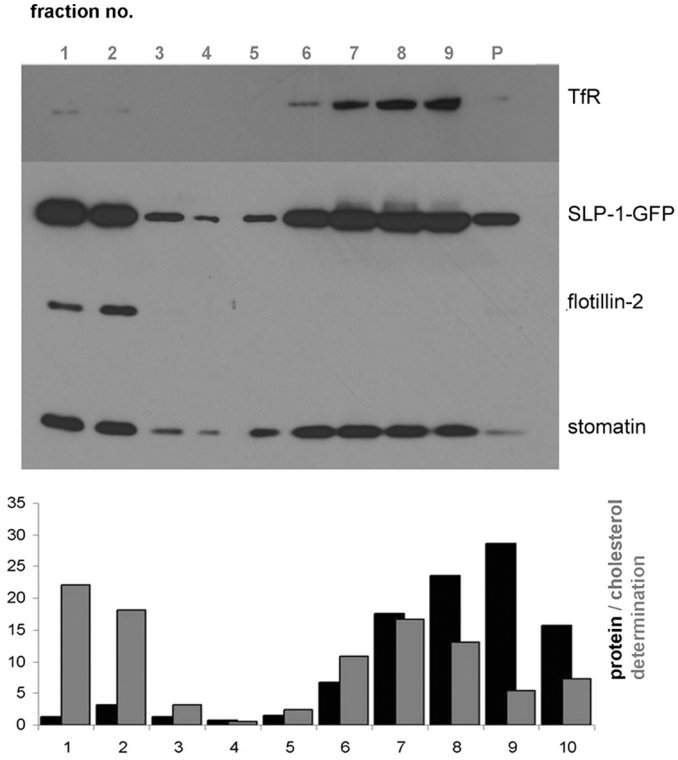

FIGURE 6. **SLP-1 is enriched in lipid rafts/DRMs.** DRM isolation from HeLa cells stably expressing SLP-1-GFP was performed as described under "Experimental Procedures." Fractions of the density gradient were analyzed by Western blotting (*upper panel*) and quantitative protein and cholesterol determination (*lower panel*). The low-density DRMs were recovered in fractions 1 and 2 at the top of the gradient. These fractions contained only 5% of the total membrane proteins but 40% of total cholesterol. Flotillin-2 and stomatin were used as DRM marker proteins. The TfR was used as a marker for non-DRM proteins and was detected in high-density fractions 6–9. A strong signal for SLP-1-GFP was found in the DRM fractions. *P*, pellet fraction.

The SLP-1 N Terminus Is Sufficient to Cause Exclusive, Late Endosomal Targeting of SLP-1/Stomatin Chimeras—The N-terminal deletion mutant of stomatin localizes like the WT to the plasma membrane and late endosomes (42). To determine whether the N terminus of SLP-1 could cause exclusive, late endosomal targeting independent of the C terminus, we fused residues 1–49 of SLP-1 to the GFP-tagged N-terminal deletion mutant of stomatin, STOM-(21–287)-GFP. Moreover, we fused the N termini containing the Y6A and L9S mutations to STOM-(21–287)-GFP and transiently transfected them into HeLa cells (supplemental Fig. S4). The cells were stained with LysoTracker Red to visualize the late endosomal compartment. As expected, STOM-(21–287)-GFP localized to the plasma membrane and LysoTracker Red-positive, perinuclear vesicles (Fig. 8, *top panel*). In striking contrast, the fusion of the SLP-1 N terminus to STOM-(21–287) resulted in the loss of plasma membrane staining and showed exclusive, late endosomal localization (Fig. 8, *second panel from top*). The chimeras with the Y6A and L9S mutations showed similar distributions as STOM-(21–287)-GFP (Fig. 8, *third* and *fourth panels*, respectively). These results demonstrate that the N terminus of SLP-1 is sufficient to cause late endosomal targeting in a similar structural context.

The SCP-2 Domain of SLP-1 Causes the Formation of Large Cholesterol-rich Vesicles upon Treatment with the Amino Steroid U18666A—To study the effect of SLP-1 expression on cholesterol distribution within the cell, we performed filipin staining of a mixture of control HeLa cells and HeLa cells stably expressing SLP-1-GFP. In both cell types, filipin weakly stained the plasma membrane and the perinuclear region showing that SLP-1-GFP expression does not substantially change the cellular cholesterol distribution (Fig. 9*A*, *upper panel*). When we treated the mixed cells with U18666A, an inhibitor of cholesterol efflux from late endosomes, we observed stronger filipin staining in perinuclear vesicles, as previously described (51, 52), however, there was a marked difference in vesicle size between the normal and transfected cells. In response to U18666A, the mean diameter of filipin-positive vesicles in normal HeLa cells increased to about 1 μm, whereas it increased to 2–3 μm in SLP-1-GFP expressing cells (Fig. 9*A*, *middle panel*). These enlarged vesicles or vacuoles were also observed in cells transiently expressing SLP-1-myc and were visible by phase-con-

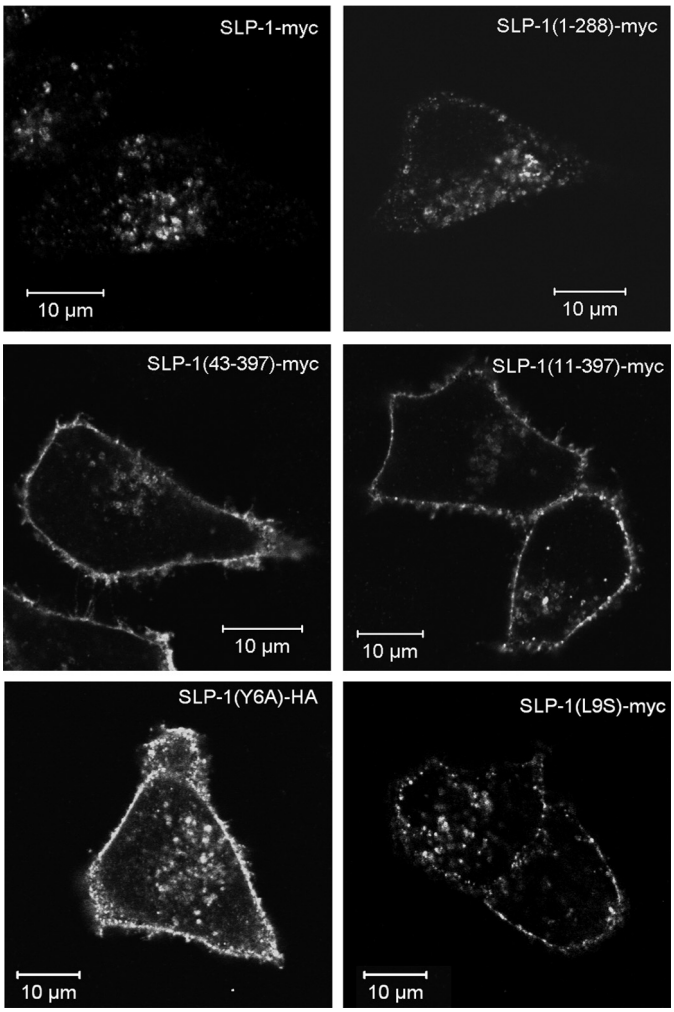

FIGURE 7. **A GY*XX*Φ motif on the N terminus of SLP-1 is essential for subcellular targeting to late endosomes.** N-terminal and C-terminal deletion constructs of SLP-1 were transiently transfected into HeLa cells and analyzed by confocal microscopy. *Upper panels*, cells expressing SLP-1-myc or SLP-1-(1–288)-myc show perinuclear staining. *Middle panels*, SLP-1-(43–397)-myc shows strong plasma membrane staining that is never observed in WT SLP-1 transfections (compare Figs. 2–4), and some perinuclear staining. SLP-1-(11–397)-myc shows the same staining pattern. *Lower panels*, point mutants SLP-1(Y6A)-HA and SLP-1(L9S)-myc are also localized to the plasma membrane thus demonstrating the essential role of the GY*XX*Φ motif for late endosomal targeting of SLP-1. *Scale bar*, 10 μm.

trast (supplemental Fig. S5). Although the cholesterol affine drug filipin apparently stained the whole lipidic content, tagged SLP-1 was distributed on the surface of these large vesicles in accordance with its localization to the limiting membrane (Fig. 2*B*). To investigate the role of the SCP-2 domain in this context, we treated a mixture of normal and SLP-1-(1–288)-GFP expressing HeLa cells with U18666A. The transfected cells showed cholesterol accumulation in perinuclear vesicles, however, the vesicle diameters were about 1 μm, such as in normal HeLa cells, and the enlarged vesicles were absent (Fig. 9*A*, *lower panel*). To quantify the phenotypic differences between the SLP-1-GFP and SLP-1-(1–288)-GFP expressing cells, we analyzed 50 cells of each cell type for maximum vesicle size in response to U18666A treatment. Almost 80% of the SLP-1-GFP expressing cells but only about 20% of the SLP-1-(1–288)-GFP expressing cells contained vesicles larger than 1.5 μm (Fig. 9*B*). These results indicate that the SCP-2 domain is responsible for formation of the large, cholesterol-filled vesicles or vacuoles when the efflux of cholesterol from late endosomes is inhibited. When we treated HeLa cells stably expressing SLP-1-(43–397)-myc, which is mainly localized to the plasma membrane (Fig. 7), with U18666A, we observed filipin-stained vesicles as in normal HeLa cells but no enlarged vesicles (data not shown). This indicates that the localization of SLP-1 to late endosomes is crucial.

The Enlarged, SLP-1-GFP-induced Vesicles Are Weakly LAMP-2-positive—When we performed triple staining fluorescence microscopy of U18666A-treated HeLa cells stably expressing SLP-1-GFP, we noticed that the enlarged, SLP-1-GFP- and filipin-positive vesicles were only weakly stained with anti-LAMP-2 (Fig. 10*A* and supplemental Fig. S6*B*), however, these vesicles were LysoTracker Red-positive (supplemental Fig. S6*C*). In control HeLa cells treated with U18666A, a large proportion of filipin-positive vesicles co-localized with LAMP-2 (supplemental Fig. S6*A*). Similarly, SLP-1-(1–288)-GFP expressing cells showed co-localization of SLP-1-(1–288)-GFP, cholesterol, and LAMP-2 (Fig. 10*B*). Despite weak LAMP-2 staining, we conclude that due to staining with LysoTracker Red, the large, SLP-1-GFP-positive vesicles or vacuoles are part of the late endosomal compartment.

DISCUSSION

Nothing is known about the molecular and cell biological characteristics of the human stomatin-like protein SLP-1 except for its bipartite structure consisting of a stomatin and SCP-2/nonspecific lipid transfer protein domain (7). In the absence of antibodies to the native protein, despite many immunization attempts, we started to investigate the subcellular localization of various tagged forms (myc, HA, and GFP) of SLP-1 in various cell lines at varying expression levels. Independent of these variations, expressed SLP-1 was always identified in perinuclear vesicles that co-localized with markers for the late endosomal/lysosomal compartment. Late endosomal targeting was further supported by immunoelectron microscopy and co-localization with acidic vesicles and endocytosed TRITC-dextran. Therefore, and because of the canonical sorting signal, GY*XX*Φ, it is most likely that the endogenous SLP-1 is also residing in the late endosomal compartment.

Stomatin localizes to the plasma membrane and the late endosomal compartment (28). Our present study shows that SLP-1 and stomatin co-localize well in late endosomes but not at the plasma membrane, which is only positive for stomatin. Interestingly, SLP-1 overexpression led to a shift in stomatin distribution from the plasma membrane to late endosomes. This regulatory effect of SLP-1 on stomatin distribution is reminiscent of but different from the situation in *C. elegans*. There, the stomatin orthologue UNC-1 is localized to the plasma membrane in the presence of the SLP-1 orthologue UNC-24; however, when UNC-24 is mutated, UNC-1 localizes to perinuclear vesicles (41). Thus, UNC-24 regulates the localization of UNC-1. Although this regulation may be similar in human cells, the localization of the human orthologues is different. The regulated co-localization nevertheless, suggests an interaction between these proteins in *C. elegans* and human cells. Moreover, the interaction of UNC-24 with stomatin-like protein

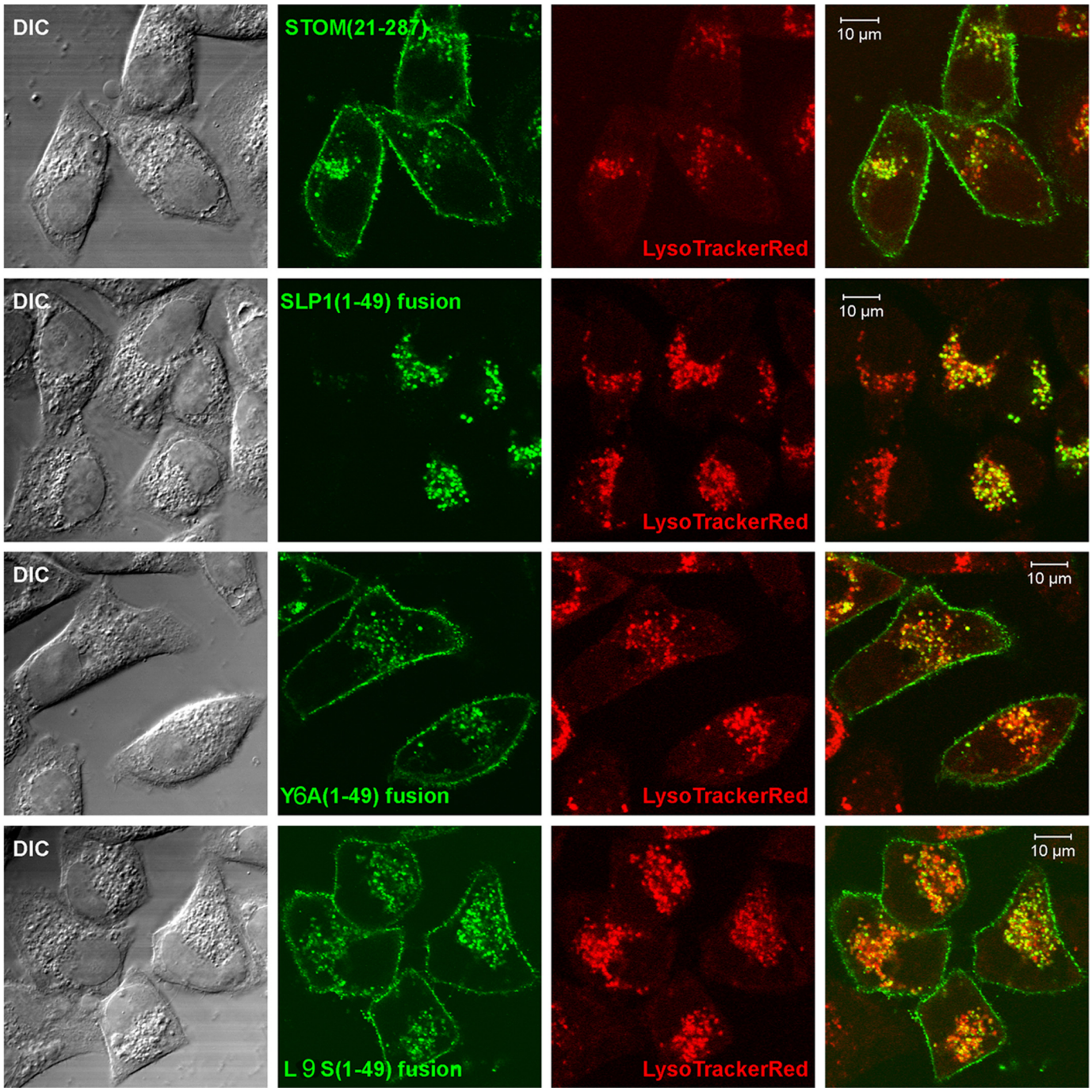

FIGURE 8. **The GY*XX*Φ motif within the N terminus of SLP-1 is sufficient to induce late endosomal localization of chimeric SLP-1/stomatin fusion proteins.** Chimeric fusion proteins, with the N terminus of stomatin being replaced by the N terminus of SLP-1, were produced as described under "Experimental Procedures." Transiently transfected cells were analyzed by fluorescence microscopy and Western blotting (see supplemental Fig. S4). Cells were stained with LysoTracker Red and confocal images of cells expressing the indicated constructs are depicted. Differential interference contrast images (*DIC*), single channel images for GFP (*green*) and LysoTracker Red (*red*), and overlay images are shown. *Top panel*, STOM-(21–287) is localized to the plasma membrane and late endosomes. *Second panel*, fusion of residues 1–49 of SLP-1 to STOM-(21–287) causes an exclusive, perinuclear localization. *Third* and *fourth panels*, introduction of the Y6A or L9S point mutations in the N terminus of SLP-1 abrogates this effect and gives rise to chimeras with a subcellular localization indistinguishable from WT stomatin and STOM-(21–287). *Scale bars*, 10 μm.

MEC-2 (36) suggests a general tendency of stomatin-like proteins to associate. We proved the postulated interaction of SLP-1 with stomatin by co-immunoprecipitation and localized the interaction site to the conserved stomatin part of SLP-1. SLP-1 does not contain a C-terminal interaction domain as described for stomatin (49) and it is currently not clear whether the hydrophobic domain, PHB domain, or the connecting region between the PHB and SCP-2 domains (residues 224–288) is responsible for interaction with stomatin. Other possible interaction sites may include the flanking residues of the respective PHB domains that are involved in trimerization of stomatin (53) or the hydrophobic domain in analogy to the caveolin-1 and -2 interaction (54). The exact interaction site remains to be identified.

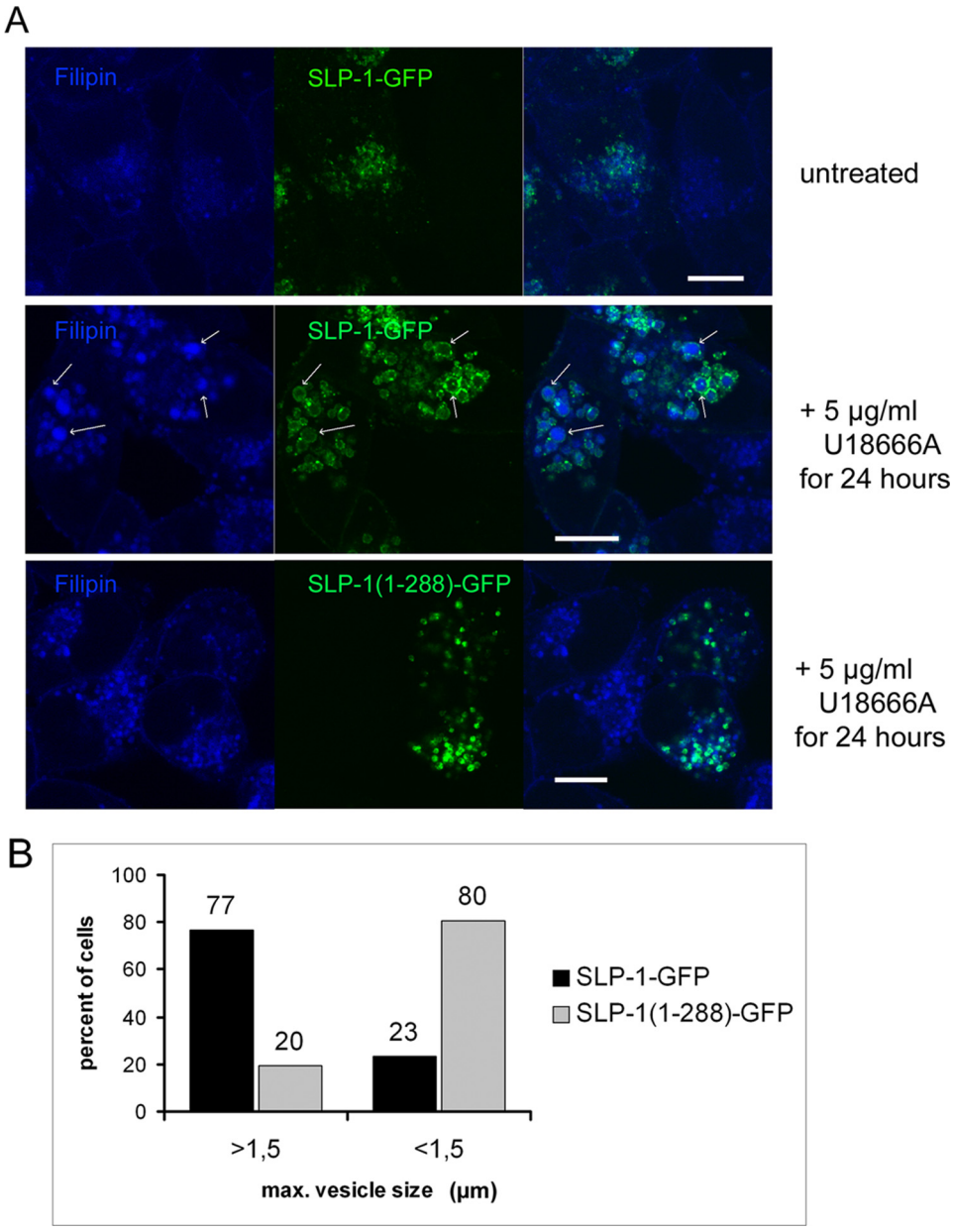

FIGURE 9. **Treatment with the amino steroid U18666A of HeLa cells stably expressing SLP-1-GFP results in the formation of large, cholesterol-rich vesicles.** *A*, *upper panel*, a mixture of control and SLP-1-GFP expressing HeLa cells was cultivated in the absence of U18666A and stained with filipin (*blue*) to visualize cholesterol distribution. Weak filipin staining was detected on the plasma membrane and in the perinuclear regions of both cell populations. *Middle panel*, mixed SLP-1-GFP expressing and normal HeLa cells were treated with U18666A as indicated. In the cells expressing SLP-1-GFP, large, filipin-stained vesicles or vacuoles can be seen (*arrows*) that are surrounded by SLP-1-GFP, whereas in normal HeLa cells, filipin-stained vesicles are clearly smaller. *Lower panel*, cells expressing SLP-1-(1–288)-GFP were treated with U18666A and analyzed in the same way. Filipin-stained, SLP-1-(1–288)-GFP-positive vesicles can be observed but not the enlarged vesicles. *Scale bars*, 10 μm. *B*, phenotypic comparison of cells expressing SLP-1-GFP or SLP-1-(1–288)-GFP after treatment with 5 μg/ml U18666A for 24 h. The diameter of the largest vesicular structures positive for the respective GFP fusion protein and filipin was measured with the software of the Zeiss LSM microscope in 50 different cells for each cell type. Diameters larger or smaller than 1.5 μm were scored. The relative percentage of cells with either large or small vesicles is shown in the diagram.

A hallmark of stomatin and similar proteins is their association with DRMs/lipid rafts. Therefore, we studied DRM association of SLP-1 and stomatin by analyzing their distribution in density gradients. SLP-1 is partially associated with DRMs and its distribution resembles that of stomatin and cholesterol. DRM association of mutants SLP-1-(1–288) and SLP-1-(1–224) suggests that the PHB domain is involved, possibly in combination with the hydrophobic domain and/or palmitoylation, as described for flotillin/reggie proteins (55–57). This property of SLP-1 is in contrast to stomatin, which loses DRM association when mutated near the C-terminal end (49).

Analysis of the N terminus of SLP-1 revealed the canonical sorting signal, G*YXX*Φ, which is essential for late endosomal targeting of integral membrane proteins like LAMP-1 and -2 (50). Deletion or mutation of this signal affected the correct targeting and led to accumulation of the respective mutants at the plasma membrane. The importance of this signal was also demonstrated by the exclusive, late endosomal targeting of a chimeric protein consisting of the WT N terminus of SLP-1 and an N-terminal deletion mutant of stomatin. Mutations within the G*YXX*Φ motif of this chimeric protein led to plasma membrane localization. These data show that an active transport mechanism is responsible for the late endosomal targeting of SLP-1, which relies on the N-terminal sorting signal. Although the Y-based sorting signals on lysosomal-associated membrane proteins are found at the extreme C terminus within a short, well defined range from the transmembrane domain (50, 58), we show here that this signal also functions at the N terminus of SLP-1. Apparently, the structure of the N-terminal region allows interaction of the signal with adapter protein complexes. Depending on the adapter, the cargo can be transported to the endosomal system either directly from the trans-Golgi network or indirectly via the plasma membrane (50). Because we never observed significant plasma membrane staining of SLP-1 in steady state, a direct transport mechanism may be suggested. However, the SLP-1-induced redistribution of stomatin from the plasma membrane to late endosomes argues for intermediary targeting of the plasma membrane. Moreover, strong staining of the plasma membrane when the Y-based signal is impaired may also argue for intermediary plasma membrane targeting of WT SLP-1. More detailed studies will have to clarify this issue.

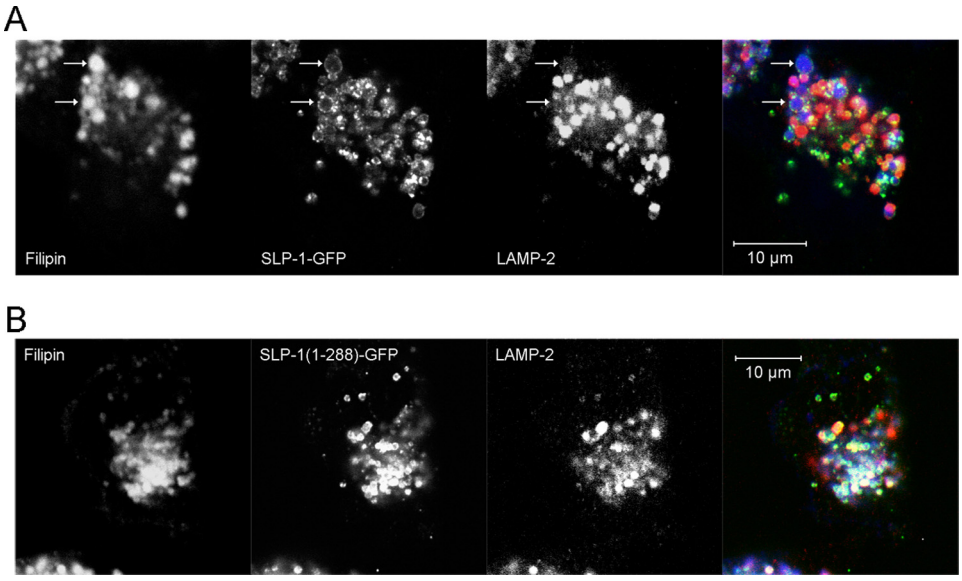

FIGURE 10. **Reduced LAMP-2 expression on the large, cholesterol-rich SLP-1-GFP-positive vesicles.** Cells stably expressing either SLP-1-GFP or SLP-1-(1–288)-GFP were treated with 3 μg/ml U18666A for 24 h. The cells were fixed and stained with filipin (*blue*) and anti-LAMP-2 antibody (*red*). *A*, the enlarged, filipin-positive vesicles that are observed in cells expressing SLP-1-GFP (*arrows*) contain very little LAMP-2. *B*, co-localization of filipin, SLP-1-(1–288)-GFP, and LAMP-2 can be clearly seen in a large part of the late endosomal compartment. Compare the triple overlays in *A* and *B*. *Scale bars*, 10 μm.

To study the effect of SLP-1 on cholesterol distribution in the cell, we analyzed the concomitant localization of SLP-1-GFP and cholesterol by filipin staining. The overexpression of SLP-1-GFP in HeLa cells did not visibly change cholesterol distribution, however, it has to be considered that there are many lipid binding and transfer proteins in the cell (17) that regulate cholesterol homeostasis (59) and therefore the gain or loss of only one such protein may not result in observable changes in cholesterol distribution. To interfere with a major pathway of cholesterol efflux from the late endosomal compartment, we treated the SLP-1-GFP expressing cells with the amino steroid U18666A, which leads to cholesterol accumulation in this compartment as in Niemann-Pick type C disease (60). Under these conditions, large, cholesterol-rich vesicles or vacuoles were formed that were much larger than those produced by the drug in normal HeLa cells. In contrast, U18666A treatment of cells expressing SLP-1-(1–288)-GFP, which is lacking the SCP-2 domain, did not show this massive effect and yielded smaller vesicles like those generated in normal HeLa cells. Thus, our data suggest that the SCP-2 domain of SLP-1 is responsible for the formation of the enlarged, cholesterol-rich vesicles. Interestingly, these vesicles showed little LAMP-2 staining but were LysoTracker Red-positive, whereas a large fraction of the SLP-1-(1–288)-GFP and filipin-stained vesicles was clearly LAMP-2-positive. It is possible that LAMP-2 is degraded by cathepsins under these cholesterol accumulating conditions, as described (61). Although the identity of the enlarged, cholesterol-rich vesicles remains to be clarified, we nevertheless, show involvement of the SCP-2 domain in their generation.

SLP-1 contains two cholesterol recognition/interaction amino acid consensus motifs (62), one in the juxtamembrane region (residues 81–86) and one in the SCP-2- domain. Cholesterol recognition/interaction amino acid consensus motifs are thought to play a role in the association of proteins with cholesterol-rich domains (63). Although cholesterol binding of the first motif has yet to be demonstrated, SCP-2 binds and transfers cholesterol, fatty acids, and other lipids (14). Our data suggest that the SCP-2 domain of SLP-1 plays a role in the transfer of cholesterol to the late endosomes, whereas specific targeting of SLP-1 is based on the G*YXX*Φ signal. Interestingly, mutation of this signal also prevents the formation of the enlarged vesicles. This may be explained by the inability of G*YXX*Φ-mutated SLP-1 to transport cholesterol to the late endosomes. In contrast to SLP-1, the late endosomal/lysosomal cholesterol-binding membrane proteins NPC1 and MLN64/MENTHO are involved in cholesterol efflux from the late endosomes back to the plasma membrane and other membranes (64, 65). Mutations of NPC1 cause inefficient cholesterol efflux and thus cholesterol accumulation in the late endosomal compartment leading to Niemann-Pick type C disease (66). Similarly, deletion of the START domain of MLN64 causes cholesterol accumulation in lysosomes (67). Diseases due to mutations of SLP-1 have not been reported to date but it may be predicted that SLP-1 dysfunction should lead to enhanced cholesterol efflux from the late endosomal compartment.

The stomatin-like proteins podocin and MEC-2 bind cholesterol and associate with ion channels in protein-cholesterol complexes thereby regulating the ion channel activity (40). Possibly, all PHB domain proteins may be involved in the formation and function of large protein-cholesterol complexes in membranes. Other proteins with a similar topology like caveolins, flotillin/reggie proteins, and reticulons may function as regulated, oligomeric, integral coat proteins with high affinity for particular lipids, thereby creating lipid microdomains (68). In addition to the structural features of these proteins, SLP-1 has a domain that is thought to be involved in cholesterol/lipid transfer. Our data are in line with this concept and suggest that SLP-1 is involved in membrane trafficking and cytoplasmic lipid distribution.

Acknowledgment—We are grateful to Ellen Umlauf for providing stomatin-GFP, STOM-(21–287)-GFP, and GFP-Rab7 constructs.

REFERENCES

1. Gilles, F., Glenn, M., Goy, A., Remache, Y., and Zelenetz, A. D. (2000) *Eur. J. Haematol.* **64,** 104–113
2. Green, J. B., and Young, J. P. (2008) *BMC Evol. Biol.* **8,** 44
3. Smith, M., Filipek, P. A., Wu, C., Bocian, M., Hakim, S., Modahl, C., and Spence, M. A. (2000) *Am. J. Med. Genet.* **96,** 765–770
4. Hiebl-Dirschmied, C. M., Entler, B., Glotzmann, C., Maurer-Fogy, I., Stratowa, C., and Prohaska, R. (1991) *Biochim. Biophys. Acta* **1090,** 123–124

5. Hiebl-Dirschmied, C. M., Adolf, G. R., and Prohaska, R. (1991) *Biochim. Biophys. Acta* **1065,** 195–202
6. Stewart, G. W., Hepworth-Jones, B. E., Keen, J. N., Dash, B. C., Argent, A. C., and Casimir, C. M. (1992) *Blood* **79,** 1593–1601
7. Seidel, G., and Prohaska, R. (1998) *Gene* **225,** 23–29
8. Wang, Y., and Morrow, J. S. (2000) *J. Biol. Chem.* **275,** 8062–8071
9. Kobayakawa, K., Hayashi, R., Morita, K., Miyamichi, K., Oka, Y., Tsuboi, A., and Sakano, H. (2002) *J. Neurosci.* **22,** 5931–5937
10. Goldstein, B. J., Kulaga, H. M., and Reed, R. R. (2003) *J. Assoc. Res. Otolaryngol.* **4,** 74–82
11. Boute, N., Gribouval, O., Roselli, S., Benessy, F., Lee, H., Fuchshuber, A., Dahan, K., Gubler, M. C., Niaudet, P., and Antignac, C. (2000) *Nat. Genet.* **24,** 349–354
12. Tavernarakis, N., Driscoll, M., and Kyrpides, N. C. (1999) *Trends Biochem. Sci.* **24,** 425–427
13. Morrow, I. C., and Parton, R. G. (2005) *Traffic* **6,** 725–740
14. Schroeder, F., Atshaves, B. P., McIntosh, A. L., Gallegos, A. M., Storey, S. M., Parr, R. D., Jefferson, J. R., Ball, J. M., and Kier, A. B. (2007) *Biochim. Biophys. Acta* **1771,** 700–718
15. Wirtz, K. W. (2006) *FEBS Lett.* **580,** 5436–5441
16. Barnes, T. M., Jin, Y., Horvitz, H. R., Ruvkun, G., and Hekimi, S. (1996) *J. Neurochem.* **67,** 46–57
17. Holthuis, J. C., and Levine, T. P. (2005) *Nat. Rev. Mol. Cell Biol.* **6,** 209–220
18. Salzer, U., Mairhofer, M., and Prohaska, R. (2007) *Dyn. Cell Biol.* **1,** 20–33
19. Stewart, G. W. (2004) *Curr. Opin. Hematol.* **11,** 244–250
20. Bruce, L. J., Guizouarn, H., Burton, N. M., Gabillat, N., Poole, J., Flatt, J. F., Brady, R. L., Borgese, F., Delaunay, J., and Stewart, G. W. (2009) *Blood* **113,** 1350–1357
21. Fricke, B., Argent, A. C., Chetty, M. C., Pizzey, A. R., Turner, E. J., Ho, M. M., Iolascon, A., von Düring, M., and Stewart, G. W. (2003) *Blood* **102,** 2268–2277
22. Fricke, B., Parsons, S. F., Knöpfle, G., von Düring, M., and Stewart, G. W. (2005) *Br. J. Haematol.* **131,** 265–277
23. Simons, K., and Toomre, D. (2000) *Nat. Rev. Mol. Cell Biol.* **1,** 31–39
24. Simons, K., and Vaz, W. L. (2004) *Annu. Rev. Biophys. Biomol. Struct.* **33,** 269–295
25. London, E., and Brown, D. A. (2000) *Biochim. Biophys. Acta* **1508,** 182–195
26. Galbiati, F., Razani, B., and Lisanti, M. P. (2001) *Cell* **106,** 403–411
27. Foster, L. J., De Hoog, C. L., and Mann, M. (2003) *Proc. Natl. Acad. Sci. U.S.A.* **100,** 5813–5818
28. Snyers, L., Umlauf, E., and Prohaska, R. (1999) *Eur. J. Cell Biol.* **78,** 802–812
29. Schwarz, K., Simons, M., Reiser, J., Saleem, M. A., Faul, C., Kriz, W., Shaw, A. S., Holzman, L. B., and Mundel, P. (2001) *J. Clin. Invest.* **108,** 1621–1629
30. Huber, T. B., Simons, M., Hartleben, B., Sernetz, L., Schmidts, M., Gundlach, E., Saleem, M. A., Walz, G., and Benzing, T. (2003) *Hum. Mol. Genet.* **12,** 3397–3405
31. Langhorst, M. F., Reuter, A., and Stuermer, C. A. (2005) *Cell Mol. Life Sci.* **62,** 2228–2240
32. Price, M. P., Thompson, R. J., Eshcol, J. O., Wemmie, J. A., and Benson, C. J. (2004) *J. Biol. Chem.* **279,** 53886–53891
33. Zhang, J. Z., Hayashi, H., Ebina, Y., Prohaska, R., and Ismail-Beigi, F. (1999) *Arch. Biochem. Biophys.* **372,** 173–178
34. Zhang, J. Z., Abbud, W., Prohaska, R., and Ismail-Beigi, F. (2001) *Am. J. Physiol. Cell Physiol.* **280,** C1277–C1283
35. Montel-Hagen, A., Kinet, S., Manel, N., Mongellaz, C., Prohaska, R., Battini, J. L., Delaunay, J., Sitbon, M., and Taylor, N. (2008) *Cell* **132,** 1039–1048
36. Zhang, S., Arnadottir, J., Keller, C., Caldwell, G. A., Yao, C. A., and Chalfie, M. (2004) *Curr. Biol.* **14,** 1888–1896
37. Huang, M., Gu, G., Ferguson, E. L., and Chalfie, M. (1995) *Nature* **378,** 292–295
38. Morgan, P. G., Sedensky, M., and Meneely, P. M. (1990) *Proc. Natl. Acad. Sci. U.S.A.* **87,** 2965–2969
39. Rajaram, S., Sedensky, M. M., and Morgan, P. G. (1998) *Proc. Natl. Acad. Sci. U.S.A.* **95,** 8761–8766
40. Huber, T. B., Schermer, B., Müller, R. U., Höhne, M., Bartram, M., Calixto, A., Hagmann, H., Reinhardt, C., Koos, F., Kunzelmann, K., Shirokova, E., Krautwurst, D., Harteneck, C., Simons, M., Pavenstädt, H., Kerjaschki, D., Thiele, C., Walz, G., Chalfie, M., and Benzing, T. (2006) *Proc. Natl. Acad. Sci. U.S.A.* **103,** 17079–17086
41. Sedensky, M. M., Siefker, J. M., and Morgan, P. G. (2001) *Am. J. Physiol. Cell Physiol.* **280,** C1340–C1348
42. Umlauf, E., Csaszar, E., Moertelmaier, M., Schuetz, G. J., Parton, R. G., and Prohaska, R. (2004) *J. Biol. Chem.* **279,** 23699–23709
43. Steiner, M., Schöfer, C., and Mosgoeller, W. (1994) *Histochem. J.* **26,** 934–938
44. Meyers, J. M., and Prekeris, R. (2002) *J. Biol. Chem.* **277,** 49003–49010
45. Lowry, O. H. (1957) *Methods Enzymol.* **4,** 366–381
46. Bonifacino, J. S., and Dell'Angelica, E. C. (2001) in *Current Protocols in Cell Biology* (Bonifacino, J. S., Dasso, M., Harford, J. B., Lippincott-Schwartz, J., and Yamada, K. M., eds) Unit 7.2, John Wiley & Sons, Inc., New York
47. Kobayashi, T., Beuchat, M. H., Lindsay, M., Frias, S., Palmiter, R. D., Sakuraba, H., Parton, R. G., and Gruenberg, J. (1999) *Nat. Cell. Biol.* **1,** 113–118
48. Snyers, L., Thinès-Sempoux, D., and Prohaska, R. (1997) *Eur. J. Cell Biol.* **73,** 281–285
49. Umlauf, E., Mairhofer, M., and Prohaska, R. (2006) *J. Biol. Chem.* **281,** 23349–23356
50. Bonifacino, J. S., and Traub, L. M. (2003) *Annu. Rev. Biochem.* **72,** 395–447
51. Tomiyama, Y., Waguri, S., Kanamori, S., Kametaka, S., Wakasugi, M., Shibata, M., Ebisu, S., and Uchiyama, Y. (2004) *Cell Tissue Res.* **317,** 253–264
52. Sobo, K., Le Blanc, I., Luyet, P. P., Fivaz, M., Ferguson, C., Parton, R. G., Gruenberg, J., and van der Goot, F. G. (2007) *PLoS ONE* **2,** e851
53. Yokoyama, H., Fujii, S., and Matsui, I. (2008) *J. Mol. Biol.* **376,** 868–878
54. Das, K., Lewis, R. Y., Scherer, P. E., and Lisanti, M. P. (1999) *J. Biol. Chem.* **274,** 18721–18728
55. Morrow, I. C., Rea, S., Martin, S., Prior, I. A., Prohaska, R., Hancock, J. F., James, D. E., and Parton, R. G. (2002) *J. Biol. Chem.* **277,** 48834–48841
56. Neumann-Giesen, C., Falkenbach, B., Beicht, P., Claasen, S., Lüers, G., Stuermer, C. A., Herzog, V., and Tikkanen, R. (2004) *Biochem. J.* **378,** 509–518
57. Liu, J., Deyoung, S. M., Zhang, M., Dold, L. H., and Saltiel, A. R. (2005) *J. Biol. Chem.* **280,** 16125–16134
58. Rohrer, J., Schweizer, A., Russell, D., and Kornfeld, S. (1996) *J. Cell Biol.* **132,** 565–576
59. Ikonen, E. (2008) *Nat. Rev. Mol. Cell Biol.* **9,** 125–138
60. Liscum, L., and Faust, J. R. (1989) *J. Biol. Chem.* **264,** 11796–11806
61. Bandyopadhyay, U., Kaushik, S., Varticovski, L., and Cuervo, A. M. (2008) *Mol. Cell. Biol.* **28,** 5747–5763
62. Epand, R. F., Thomas, A., Brasseur, R., Vishwanathan, S. A., Hunter, E., and Epand, R. M. (2006) *Biochemistry* **45,** 6105–6114
63. Epand, R. M. (2006) *Prog. Lipid Res.* **45,** 279–294
64. Infante, R. E., Wang, M. L., Radhakrishnan, A., Kwon, H. J., Brown, M. S., and Goldstein, J. L. (2008) *Proc. Natl. Acad. Sci. U.S.A.* **105,** 15287–15292
65. Alpy, F., and Tomasetto, C. (2006) *Biochem. Soc. Trans.* **34,** 343–345
66. Scott, C., and Ioannou, Y. A. (2004) *Biochim. Biophys. Acta* **1685,** 8–13
67. Zhang, M., Liu, P., Dwyer, N. K., Christenson, L. K., Fujimoto, T., Martinez, F., Comly, M., Hanover, J. A., Blanchette-Mackie, E. J., and Strauss, J. F., 3rd (2002) *J. Biol. Chem.* **277,** 33300–33310
68. Bauer, M., and Pelkmans, L. (2006) *FEBS Lett.* **580,** 5559–5564